Research Article

BIOMEDICAL Journal of Scientific & Technical Research

ISSN: 2574 -1241

DOI: 10.26717/BJSTR.2022.46.007294

Synthesized Biomaterial is Potential Candidate for Cancer Therapy & NUV LED Chips

Sanjay Kumar Dubey[1] and Shashank Sharma[2]*

[1]*Department of Physics, Dr. Radha Bai, Govt. Navin Girls College, India*

[2]*Department of Physics, Dr. C. V. Raman University, India*

***Corresponding author:** Shashank Sharma, Department of Physics, Dr. C. V. Raman University, Kota, Bilaspur (Chhattisgarh), India

ARTICLE INFO

Received: August 24, 2022

Published: September 09, 2022

Citation: Sanjay Kumar Dubey and Shashank Sharma. Synthesized Biomaterial is Potential Candidate for Cancer Therapy & NUV LED Chips. Biomed J Sci & Tech Res 46(1)-2022. BJSTR. MS.ID.007294.

Abbreviations: XRD: X-ray Diffraction; FTIR: Fourier Transform Infra-Red Spectroscopy; PL: Photoluminescence; WLEDs: White Light Emitting Diodes; Ca: Calcium; Ba: Barium; Sr: Strontium; NUV: Near Ultraviolet; UV: Ultraviolet; Eu: Europium; Dy: Dysprosium; Ce: Cerium; CH3COCH3: Acetone; UDM: Uniform Deformation Model

ABSTRACT

Europium activated Ba2MgSi2O7 phosphor was synthesized via combustion synthesis technique and bluish-green emission was observed under near-ultraviolet region. The results of the XRD patterns have clearly revealed that its monoclinic crystal structure with a space group C2/c. The average crystallite size (D) is calculated as 70nm, and crystal lattice strain is also calculated as 0.27nm. The actual formation and functional group identification was clarified by FTIR spectroscopy. In PL spectra, the emission spectrum displays a single intense band allocated at 498nm wavelength, which corresponds to the 4f65d1 → 4f7 transitions of Eu2+ ions. The phosphor has shown main broad excitation peak located at 351nm, respectively. All excitation bands correspond to the allowed f→d transition of Eu2+ ions. The PL excitation spectra and comparison of PL emission spectra shown displays maximum intensity when Eu is 5mol% after that concentration quenching of Eu2+ occurs which results in decrease in PL intensity. The pairing or coagulation of activator ions may have created quenching centres, seems to be the reason for decrease in intensity after a specific concentration of Eu2+ ions. The calculated colour-chromaticity coordinate that this [X = 0.2513, Y = 0.6113] co-ordinate represents the green light emission from the phosphor. The favorable properties for the applications such as NUV-LED conversion phosphor, white light emitting diode and detection of cancer disease.

Keywords: XRD; FTIR; PL; Monoclinic; Combustion Synthesis; NUV-LED

Introduction

All over the world, material science research has done phenomenal work in the field of lighting, which has made researchers more aware and diligent in the investigation for white light emitting phosphor. That is, it will not be an exaggeration to call WLEDs the 5th generation lighting source. Nowadays, the silicate-based phosphors are widely investigated as favorable luminescent materials because of their attractive and unique features. The alkaline earth (i.e., Ca, Ba, Sr) silicates have relatively remarkable stability of physical and chemical features, as well as crystalline structure [1-4]. Silicates possess extreme chemical resistance and visible light transparency and are therefore included in an attractive class of inorganic materials utilized for extensive range of applications [5]. In addition, lanthanide ion (Eu, Dy, Ce) doped alkaline earth silicates yield much better characteristics as compared to the conventional sulphide and aluminate materials used earlier, because of their high thermal and chemical stability in ambient environment, excellent

water resistance, stable crystal structure [6], brighter luminosity, cheaper, easily prepared and strong absorption in the NUV region [7]. Divalent europium [Eu^{2+}] ($4f^7$) ion exhibits different parity-allowed 4f–5d emission in different color bands from ultraviolet (UV) region depending on the host lattice in terms of site size, site symmetry and its coordination number [8,9]. $Ba_2MgSi_2O_7$ phosphor has can be an excellent host material in which the probability of the excitation energy to be trapped by the killer center is lower [10].

As a commercial phosphor, $BaMgAl_{10}O_{17}$: Eu^{2+} has been successfully prepared by this technique [11]. TTH Tam, et al. [12] have investigated that the optical characteristics of green emitting $Ba_2MgSi_2O_7$:Eu^{2+} phosphor [12]. Jing Yan, et al. [13] have investigated the PL properties of $Ba_2MgSi_2O_7$:Eu^{2+} phosphor shows the green luminescence as a result of the electric dipole-allowed transition from the lowest level of the excited $4f^65d^1$ configuration to the $4f^7$ ($^8S_{7/2}$) ground state [13]. Shanshan Yao, et al. [14] have also studied that a blue–green emitting $Ba_2MgSi_2O_7$:Eu^{2+} phosphor prepared by the combustion-assisted synthesis and an efficient bluish-green emission under from ultraviolet to visible light [14]. Thomas Aitasalo, et al. [15] have reported the monoclinic $Ba_2MgSi_2O_7$:Eu^{2+}, UV excited and persistent luminescence are observed at the green region centered at 505 nm [15]. Therefore, it is also considered and highly applicable to be a new favorable solid-state lighting device, promising candidate of white light emitting diodes and long persistent applications. Biomaterials literally means a living organism bio active molecule in vitro and vivo, used in tissue engineering [16]. Nowadays, the luminescence properties of biomaterials may be potentially applied in the drug delivery, cancer disease therapy fields, Bone Materials, Biomaterials, Bone Tissue Engineering and Tissue Engineering applications and at the same time, it is also making an important contribution to DNA transplantation and Image processing in computer science applications etc. To the best our knowledge, $Ba_2MgSi_2O_7$:Eu^{2+} phosphor is potential applicable as a bluish-green phosphor, which was observed under near-ultraviolet region. Here we report on the synthesis and characterization of bluish-green emitting $Ba_2MgSi_2O_7$:Eu^{2+} phosphor by a combustion synthesis method and investigate their luminescent properties.

Experimental and Characterization Study

Sample Synthesization Analysis

We have applied combustion synthesis process in our experiment for the preparation of $Ba_{2-x}MgSi_2O_7$: Eu_x^{2+} (5mol %) phosphor. Phosphors were prepared by combustion synthesis. The ingredients used were Ba $(NO_3)_2$.xH_2O, Mg $(NO_3)_2$.xH_2O, silicic acid (SiO_2.xH_2O) and Eu $(NO_3)_3$.xH_2O as starting raw reagents with 99.99% purity. The combustion fuel was used as urea and boric acid was used as an oxidizer. In our experiment, all constituents with appropriate molar ratios in the stated proportions, along with the combustion fuel and oxidizers, were mixed together and a very little quantity of acetone (CH_3COCH_3) was added to get a clear solution. After thoroughly grinding, the mixture was transferred to a pre-heated furnace at 650°C. On rapid heating the mixture evaporates and ignites to yield a white product. The entire combustion process is over within a few minutes. Within a few minutes, the mixture solution undergoes thermal dehydration with liberation of gaseous products, to formation of silicates and ignites to produce a self-propagating flame. The powder so obtained was annealed at 1000oC for 1 hour in a covered crucible under reducing atmosphere provided by burning charcoal. The resulting specimen was restored in airtight bottle for characterization investigations.

The chemical reaction of this entire process as follows:

$$Ba(NO_3)_2 + Mg(NO_3)_2 + SiO_2 * H_2O + NH_2CONH_2 + H_3BO_3 \rightarrow Ba_2MgSi_2O_7 + H_2O(\uparrow) + CO_2(\uparrow) + N_2(\uparrow) \quad (1)$$

$$Ba(NO_3)_2 + Mg(NO_3)_2 + SiO_2 * H_2O + Eu(NO_3)_3 + NH_2CONH_2 + H_3BO_3 \rightarrow Ba_2MgSi_2O_7 : Eu^{2+} + H_2O(\uparrow) + CO_2(\uparrow) + N_2(\uparrow) \quad (2)$$

For the combustion process of oxides, metal nitrates are applied as oxidizer and urea is also applied as a reducer [17]. With the calculation of oxidizer to fuel ratio, the elements were assigned formal valences as follows: Ba = +2, Mg = +2, Eu = +3, Si = +4, B = +3, C = +4, H = +1, O= –2, and N = 0. Such a way, the heat of combustion is maximum for Oxidizer/Fuel ratio is equal to 1 [18,19].

Sample Characterization Analysis

To confirm the structure of the synthesized phosphors, powder photographs were noted with the help of Bruker D8 advance X-ray diffractometer with Cu-K_α radiation having wavelength (λ = 1.5406 Å) at 40 kV tube voltage and 40 mA tube current. The XRD patterns collected in the range of $10° \leq 2\theta \leq 80°$ and FTIR spectra was recorded with the help of Bruker Alpha Fourier Transform Infra-Red Spectroscopy. Photoluminescence spectra were measured with a spectro-fluorophotometer (SHIMADZU, RF-5301 PC) using a xenon lamp of power 150 watt as excitation source with spectral slit width of 1.5 nm in the range 300– 650nm. All experiments were performed in identical conditions. All measurements recorded at the room temperature.

Results and Discussion

X-Ray Diffraction (XRD) Analysis

In order to determine the phase structure, crystalline size, lattice constant powder XRD analysis has been carried out. The XRD patterns of $Ba_2MgSi_2O_7$:Eu^{2+} for 5 moles% of $Ba_2MgSi_2O_7$ are shown in Figure 1. It was recorded in the range between (10^0\2θ\$80^0$). All the peaks displayed well matched with the help of standard JCPDS PDF file No. 23-0842 [20]. The layered structure, with the following cell parameters: a = 8.4128 Å, b = 10.7101 Å, c = 8.4387 Å, β = 110.71°, consists of discrete $[Si_2O_7]^{6-}$ units connected by tetrahedral coordinated Mg^{2+} and eight-coordinated Ba^{2+} ions [21]. It is generally agreed through investigations that the influence of doping doesn't affect the phase structure of the phosphors. We have

suggested that the Europium [Eu^{2+}] ion is requisite to capture the barium [Ba^{2+}] ion sites in $Ba_2MgSi_2O_7$ host crystal lattice site. The as-synthesized phosphor had better crystallinity and very good diffraction patterns were obtained.

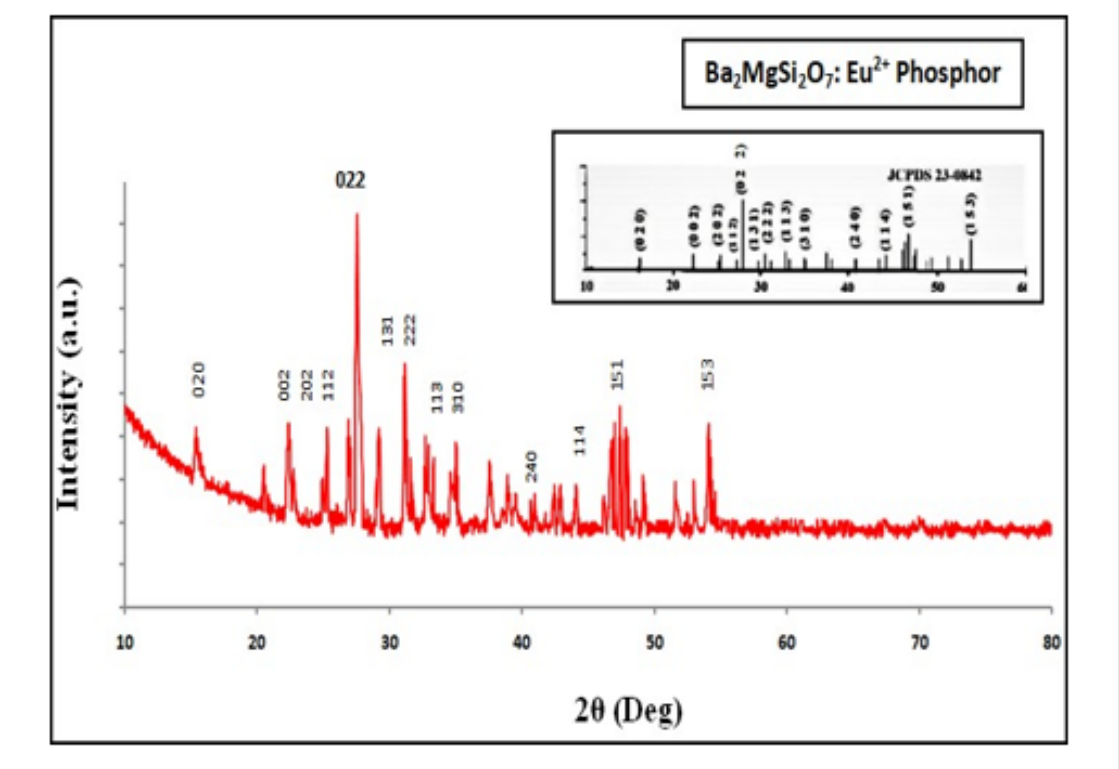

Figure 1: XRD Pattern of Synthesized Ba2MgSi2O7: Eu2+ Phosphor.

Crystallite Size Determination by Debye–Scherrer formula: Debye–Scherrer formula is represented as: D=Kλ/βCosθ, where these parameters represent, crystallite size [D] for (hkl) surface, Scherer's constant (k = 0.94 or 1) and λ is the wavelength of the incident X-ray radiation [Cu-Kα (0.15406 nm)], β (in radians) [β = 1 ($2\theta_2 - 2\theta_1$)] denotes the FWHM [Full Width at Half Maximum] of one of the primordial peaks scattered at an angle of θ is the corresponding diffraction angle for the (hkl) surface. Sharper and isolated diffraction peaks such as 2θ = 22.42 (002), 27.51 (022), 29.22 (131), 31.16 (222), 32.69 (113), 54.14 (153) were chosen for calculation of the crystallite size. Based on the Debye-Scherrer's formula, the crystallite size is ~79 nm, 76nm, 70 nm, 69 nm, 66 nm, 65 nm was calculated, respectively and the average crystallite size is ~70.00 nm.

Crystal Lattice Strain Determination by W-H Uniform Deformation Model (UDM): The strain induced broadening in the powder material was calculated via the following mathematical relation given as below:

$$\varepsilon = \beta / 4tan\theta \quad (4)$$

The crystal lattice strain was calculated from the width of prominent peak at (2θ ~ 27.51) with respect to (022) plane [19]. The relevant crystal strain size is ~ 0.27nm was evaluated with the help of the UDM. Where ε is represent the crystal lattice strain. Sharper and isolated diffraction peaks such as 2θ = 22.42 (002), 27.51 (022), 29.22 (131), 31.16 (222), 32.69 (113), 54.14 (153) were chosen for calculation of the crystal lattice strain. Based on UDM, the crystal lattice strain size is ~ 0.30nm, 0.29nm, 0.28nm, 0.27nm, 0.26nm, 0.24nm was calculated, respectively and the average crystal lattice strain size is ~ 0.27nm.

FTIR Spectra Analysis

FTIR is a non-involving damage, facile and molecular-spectroscopic technical system utilized for collecting the IR [infra-red] absorption spectrum of the phosphors [22]. Actual formation of this phosphor was obtained through FTIR. An FTIR spectrum was recorded with the help of Bruker Alpha Fourier Transform Infra-Red Spectroscopy. For investigating the functional groups (4000 to 1400 cm^{-1}) as well as the fingerprint area (1400 to 400 cm^{-1}) of synthesized phosphor through mixing the sample with analytical grade potassium bromide (KBr) with pallet preparation. The FTIR spectrum of this synthesized sample has been showed in Figure 2. The band, centered at 474.62 cm^{-1}, 567.49 cm^{-1}, 616.39 cm^{-1}, 674.39 cm^{-1}, 839.62 cm^{-1}, 929.57 cm^{-1} and 1026.23 cm^{-1} can be allocated to the responsible of silicate [SiO_4] functional group. In addition, consid-

ering the absorption bands, validated at 674.39 cm^{-1} and 567.49 cm^{-1}, respectively, because of the responsible of [SiO_4] functional group. Thus examined, the absorption bands of silicate [SiO_4] functional groups were clearly evident in the (IR) infra-red spectrum [23]. The sharp band centered at 839.62, 929.57 cm^{-1} and 1026.23cm^{-1} was allocated because of the responsible of Si-O-Si asymmetric stretch. The bands allocated at 674.39 cm^{-1} and 616.93 cm^{-1} may be responsible due to the [Si-O] symmetric stretching and [Ba-O] bending vibrations. The bands bending revealed at 567.49 cm^{-1} and 474.62 cm^{-1}, because of the existence of [Si-O- Si] vibrational mode [24]. The Peak centered at 839.62 cm^{-1} may be responsible to [Mg-O] bending vibrations and due to the asymmetric stretching on its spectrum dominates, band allocated at 1652.45 cm^{-1}. The bands centered at 1823.42 cm^{-1}, 1873.66 cm^{-1} and 1968.33 cm^{-1} is responsible because of the carbonation reaction mechanism. This can be led to distortion in the lattice resulting in 1436.79 cm^{-1} and 1652.45 cm^{-1} vibration modes represented to vibration in divalent barium ion [Ba^{2+}] and divalent magnesium ion [Mg^{2+}], respectively [24,25]. At 3475.51 cm^{-1}, peak centered due to [O-H] hydroxyl group stretching which reveals the inherence of moisture in this synthesized powder sample [26].

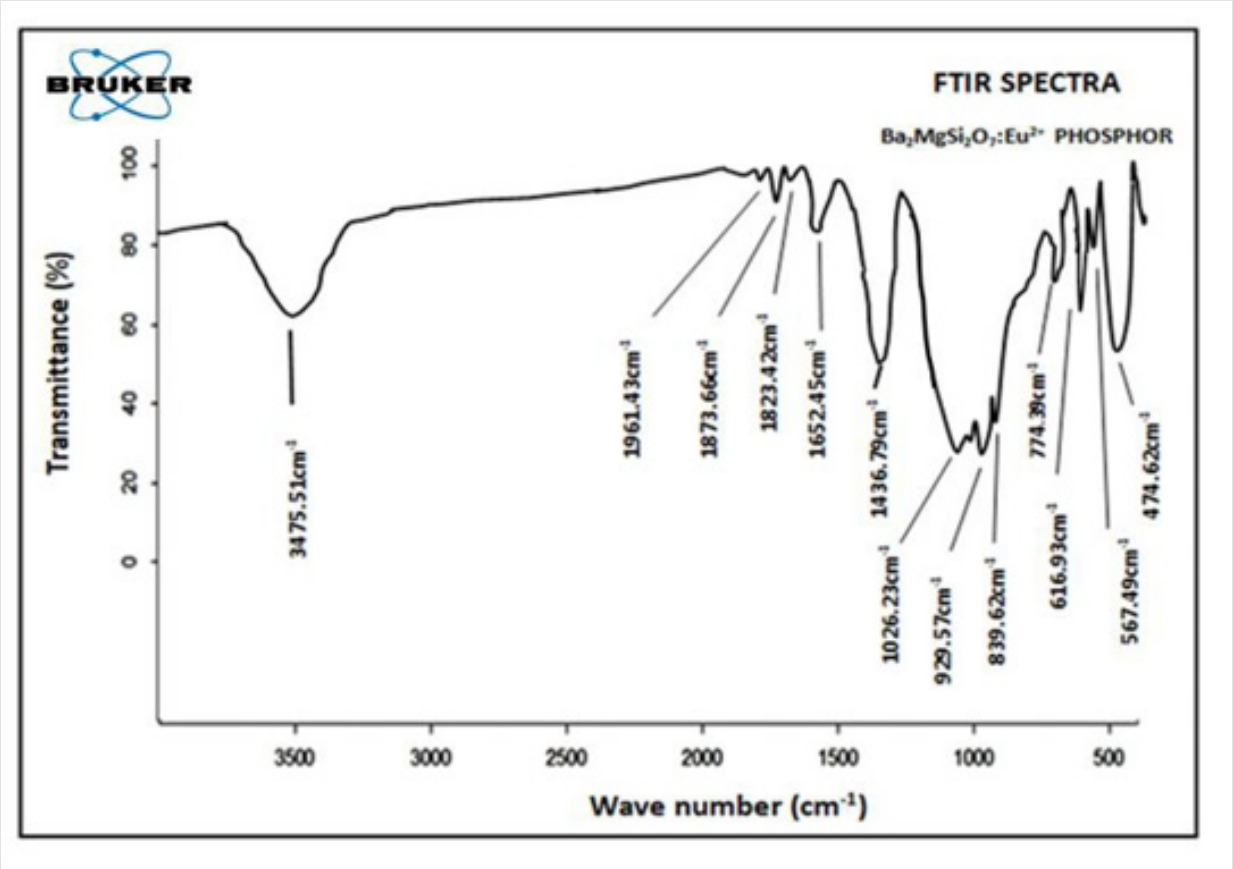

Figure 2: FTIR Spectra of Synthesized Ba2MgSi2O7: Eu2+ phosphor.

Photoluminescence Properties

The excitation and emission spectra display in Figure 3, respectively. For the excitation spectra of 351nm, broadband emission peak obtained at 498 nm. The excitation bands originate from the $4f^6 \rightarrow 4f^7 5d^1$ transitions of Eu^{2+} ions. It can be seen that the excitation band situated at 351nm in longer wavelength region ranges. The absorption of the Eu^{2+}- doped $Ba_2MgSi_2O_7$ phosphor obtained in this work matches the excitation wavelength of the NUV LED chip applied for White LEDs. The broadband emission spectra centered at 498nm (Bluish-Green region) observed under the ultraviolet excitation of 351nm correspond to the Eu^{2+} emission due to transitions from sublevels of $4f^6 5d^1$ configuration to $^8S_{7/2}$ level of the $4f^7$ configuration. The emission spectra cover from 400 nm to 600nm, which is a sign of a good phosphor. The emission peak of the phosphor is attributed to the typical emission of divalent europium [Eu^{2+}] ion because of the $4f^6 5d^1 \rightarrow 4f^7$, which transition of Eu^{2+} ions, which is an allowed electrostatic dipole transition. With an increase in the Eu^{2+} concentration, quenching of Eu^{2+} luminescence occurs. The critical quenching concentration of Eu^{2+} ions in $Ba_2MgSi_2O_7$: Eu^{2+} phosphor is determined as 5 mol%. Figure 3 shows the dependence of Eu^{2+} emission intensity on Eu^{2+} doping concentration in $Ba_2MgSi_2O_7$ host. Excited at 351nm, $Ba_2MgSi_2O_7$: xmol%

Eu^{2+} (x = 5) phosphor show emission bands with similar shape but different emission intensities. The Eu2+ emission intensity could be increased by increasing Eu^{2+} concentration. But the Eu^{2+} emission intensity reduces after 5mol% for synthesized phosphor. The reduction of Eu2+ emission intensity is induced by concentration quenching mechanism.

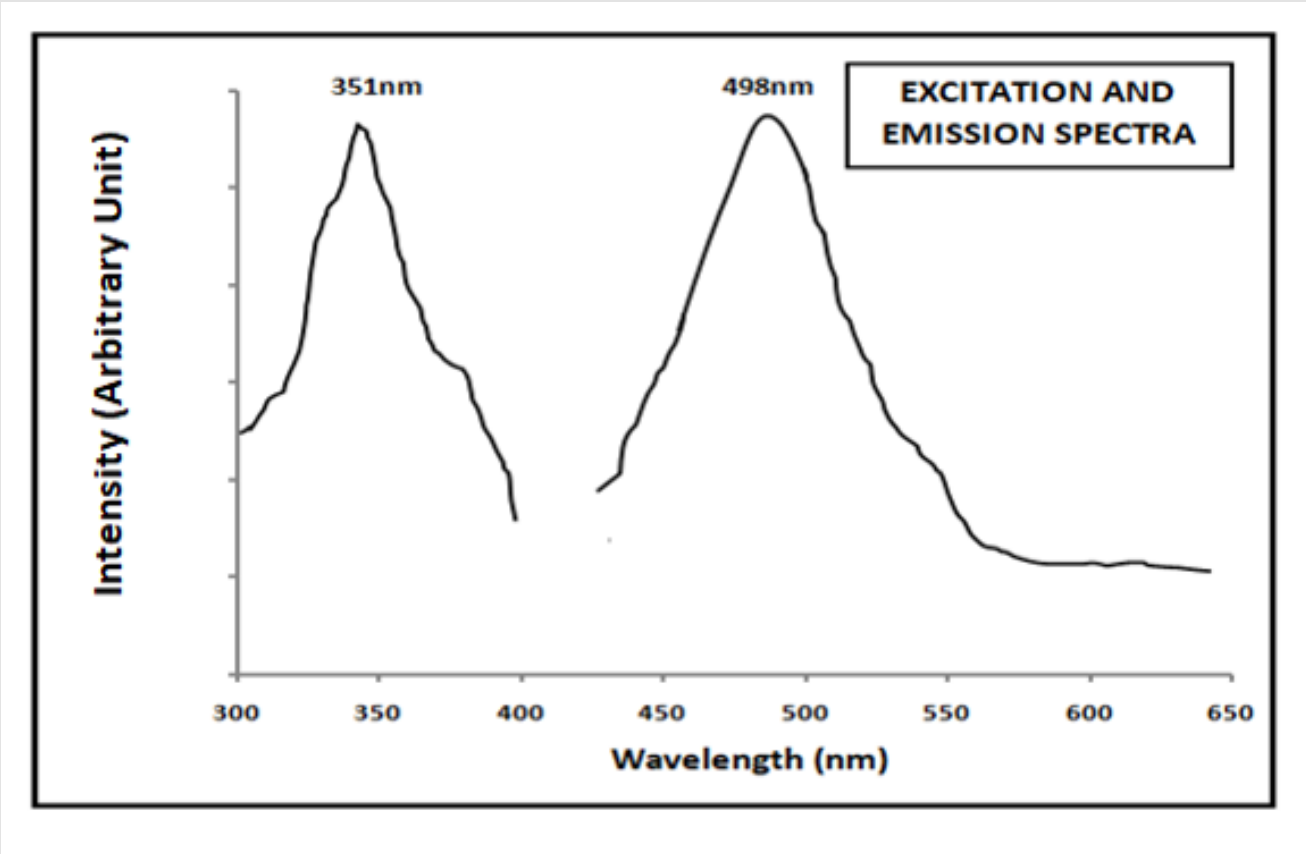

Figure 3: Excitation and Emission Spectra of Synthesized Ba2MgSi2O7: Eu2+ Phosphor.

The concentration quenching is caused by the non-radiative energy transfer between neighboring Eu^{2+} ions. No emission peaks of Eu^{3+} were observed in the spectra. This implies that the Eu^{3+} ions in the matrix had been completely reduced to Eu^{2+} in the reducing atmosphere. It is well known that the emission spectrum shows an efficient bluish-green emission under from ultraviolet to visible light which single intensive band centered at 498 nm wavelength corresponds to the transitions of $^4F_{9/2} \rightarrow {}^6H_{13/2}$ and this emission belongs to hypersensitive transition with (J = 2) [12,14]. We get information about the inter-atomic distance and ionic radii from the literature of Shannon (1976). On the basis we are suggesting that in the host $Ba_2MgSi_2O_7$ crystal structure, divalent Europium [Eu^{2+}] (1.12Å) requires to acquisition of barium cation (Ba^{2+}) site preferably. This is mainly because the ionic radius of divalent Europium [Eu^{2+}] (1.12Å) is very close to that of Barium cation (Ba^{2+}) (1.42 Å). But we also see that the ionic radius of magnesium cation (Mg^{2+}) (0.58 Å) and silicon cation (Si^{4+}) (0.26 Å) is very small. So, both these cations are far away from the reach of Europium [Eu^{2+}] ions [27]. Since the crystal field can perfectly affect the $4f^65d^1$ electron states of Eu^{2+} ions, but there is not modification in the shape of the emission spectrum therefore it is concluded that the crystal field is not changed much with the compositional variation [28,29]. Eu^{2+} ions are expected to occupy [BaO_8] sites because the coordination number of Ba^{2+} ion is eight and four for both Mg^{2+} and Si^{4+} ions. It is hard for Eu^{2+} ions to substitute the tetrahedral [MgO_4] or [SiO_4] crystal lattice symmetry but can easily substitute octahedral [BaO_8] lattice sites [30].

CIE Chromaticity Diagram

The luminescent color is the most essential and important factor for application of phosphors. Color Coordinates are the most significant factor in assessing the performance of phosphors [31]. This colour coordinate of phosphors were examined based on a clear observation of their emission spectra [32,33]. The CIE diagram of $Ba_2MgSi_2O_7$: Eu^{2+} phosphor is clearly displayed in Figure 4. It is very clear from the calculated colour- chromaticity coordinate that this [X = 0.2513, Y = 0.6113] co-ordinate represents the green light emission from the phosphor. As a result, the colour chromaticity co-ordinate of the luminescent-color emission has been displayed by this phosphor, approaches very close to green light colour region.

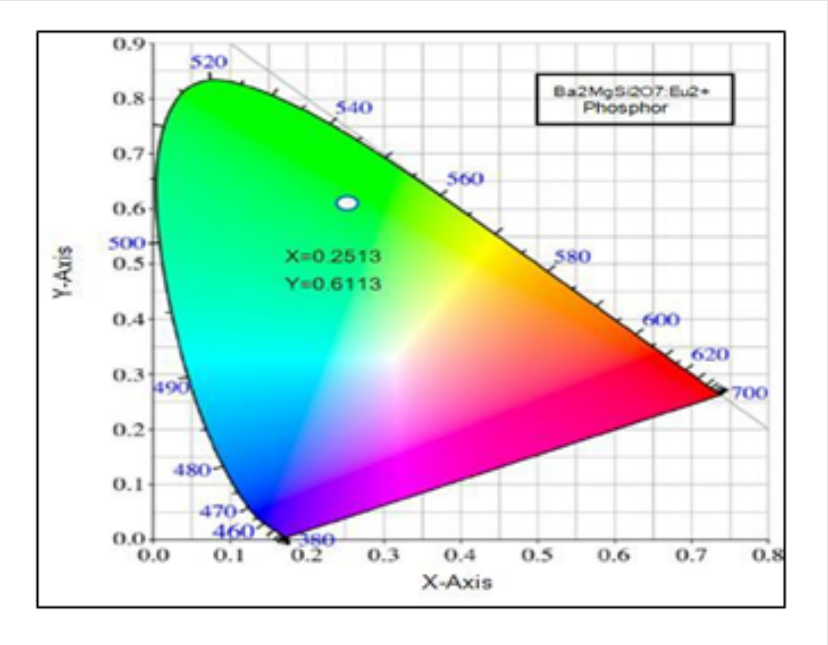

Figure 4: CIE Chromaticity Diagram of Synthesized Ba2MgSi2O7: Eu2+ Phosphor.

Conclusion

In summary, Phosphors based on $Ba_2MgSi_2O_7$: Eu^{2+} were synthesized by combustion synthesis technique, and the effects of sintering temperature on its phase and luminescent properties were investigated. At a sintering temperature of 1000°C for 1 h, the phosphors present a single monoclinic phase, and the doping ions of Eu^{2+} will clearly substitute the alkaline earth metal (Ba^{2+}) ions only slightly affects the host crystal lattice site. It is observed that all peaks of XRD pattern are well matched with the JCPDS no 23-0842, which confirms the formation of phase (monoclinic) of sample and confirmed. The average crystallite size (D) is calculated as 70nm and lattice strain as 0.27nm. Actual formation and the functional group identification of the prepared phosphor were carried out via FTIR spectroscopy. PL measurements displayed that the sintered phosphor exhibited emission peak with good intensity situated at 498nm wavelength (bluish-green emission), which was observed near UV region. With an increase in the Eu^{2+} concentration, quenching of Eu^{2+} luminescence occurs. The critical quenching concentration of Eu2+ in Ba2MgSi2O7:Eu2+ phosphor is determined as 5 mol%. The emission spectrum shows a single intense band allocated at 498 nm, which corresponds to the $4f^65d^1 \rightarrow 4f^7$ transitions of Eu^{2+} ions. The phosphor has shown main broad excitation peaks located at 351nm, respectively. The optimal PL intensity acquired with a doping concentration of 5 mol% [Eu^{2+}] ions. These results indicate that synthesized phosphor may be better promising candidate in the various field of solid-state lighting and white light long persistence phosphor as well as cancer therapy.

Acknowledgement

We gratefully acknowledge to NIT Raipur (C.G.), to the kind support for the facility of XRD analysis and FTIR analysis. Authors are also thankful to Mr. Suresh Dua and Mr. Sanjay Kumar Deshmukh NIT, Raipur (CG) India for their great co-operation at their center and Dept of physics, Pt. Ravishankar Shukla University, Raipur (C.G.) for providing us the facility of Photoluminescence analysis. The author Shashank Sharma undertakes the work of writing the entire research Paper, data collection, paper design and results-discussion. Similarly, author Sanjay Kumar Dubey has properly checked the spelling mistake and grammatical error and helped in sample preparation.

Conflict of Interest

The authors did not report any potential conflicts of economic interest exist in our present research work, authorship and/or publication of this article.

Funding

The authors have not received any financial support for the research work, authorship and and/or publication of this article.

References

1. Barry TL (1968) Fluorescence of Eu^{2+}-Activated Phases in Binary Alkaline Earth Orthosilicate Systems. Journal of the Electrochemical Society 115(11): 1181.
2. Poort SHM, Reijnhoudt HM, Van der Kuip HOT, Blasse G (1996) Luminescence of Eu^{2+} in silicate host lattices with alkaline earth ions in a row. Journal of Alloys and Compounds 241(1-2): 75-81.
3. Ju LC, Cai C, Zhu QQ, Tang JY, Hao LY, et al. (2013) Color tunable Sr_2SiO_4: Eu^{2+} phosphors through the modification of crystal structure. Journal of Materials Science: Materials in Electronics 24(11): 4516-4521.
4. Sohn KS, Cho B, Park HD (1999) Photoluminescence behavior of manganese-doped zinc silicate phosphors. Journal of the American Ceramic Society 82(10): 2779-2784.

5. Lin L, Yin M, Shi C, Zhang W (2008) Luminescence properties of a new red long-lasting phosphor: Mg_2SiO_4: Dy^{3+}, Mn^{2+}. Journal of Alloys and Compounds 455(1-2): 327-330.
6. Khan SA, Ji W, Hao L, Xu X, Agathopoulos S, et al. (2017) Synthesis and characterization of Ce^{3+}/Tb^{3+} co–doped $CaLa_4Si_3O_{13}$ phosphors for application in white LED. Optical Materials 72: 637-643.
7. Rao TGVM, Kumar AR, Veeraiah N, Reddy MR (2013) Optical and structural investigation of Sm^{3+}–Nd^{3+} co-doped in magnesium lead borosilicate glasses. Journal of Physics and Chemistry of Solids 74(3): 410-417.
8. Blasse G, Grabmaier BC (1994) A general introduction to luminescent materials. In Luminescent materials. Springer, Berlin, Heidelberg, p. 1-9.
9. Talwar GJ, Joshi CP, Moharil SV, Dhopte SM, Muthal PL, et al. (2009) Combustion synthesis of $Sr_3MgSi_2O_8$: Eu^{2+} and $Sr_2MgSi_2O_7$: Eu^{2+} phosphors. Journal of luminescence 129(11): 1239-1241.
10. Cai J, Pan H, Wang Y (2011) Luminescence properties of red-emitting $Ca_2Al_2SiO_7$: Eu^{3+} nanoparticles prepared by sol-gel method. Rare Metals 30(4): 374-380.
11. Rogachev AS, Mukasyan AS (2014) Combustion for material synthesis (1st Edn.)., CRC press.
12. Tam TTH, Du NV, Kien NDT, Thang CX, Cuong ND, et al. (2014) Co-precipitation synthesis and optical properties of green-emitting $Ba_2MgSi_2O_7$: Eu^{2+} phosphor. Journal of luminescence 147: 358-362.
13. Yan J, Ning L, Huang Y, Liu C, Hou D, et al. (2014) Luminescence and electronic properties of $Ba_2MgSi_2O_7$:Eu^{2+}: a combined experimental and hybrid density functional theory study. Journal of Materials Chemistry C 2(39): 8328-8332.
14. Yao S, Li Y, Xue L, Yan Y (2010) Photoluminescent properties of the monoclinic $Ba_2MgSi_2O_7$:Eu^{2+} phosphor prepared by the combustion-assisted synthesis method. Physica status Solidi (a) 207(9): 2164-2169.
15. Aitasalo TUOMAS, Holsa J, Laamanen TANELI, Lastusaari MIKA, Lehto LAURA, et al. (2005) Luminescence properties of Eu^{2+} doped di barium magnesium di silicate, $Ba_2MgSi_2O_7$: Eu^{2+}. Ceramics- Silikaty 49(1): 58-62.
16. Bhatkar VB, Bhatkar NV (2011) Combustion synthesis and photoluminescence study of Silicate Biomaterials. Bulletin of Materials Science 34(6): 1281-1284.
17. Ekambaram S, Maaza M (2005) Combustion synthesis and luminescent properties of Eu^{3+}-activated cheap red phosphors. Journal of alloys and compounds 395(1-2): 132-134.
18. Kingsley JJ, Patil KC (1988) A novel combustion process for the synthesis of fine particle α-alumina and related oxide materials. Materials letters 6(11-12): 427- 432.
19. Dubey SK, Sharma S, Pandey S, Diwakar AK (2021) Novel White Light Emitting ($Ba_2MgSi_2O_7$: Dy^{3+}) Phosphor. JMSRR 8(4): 172-179.
20. JCPDS Pdf file number 23-0842, JCPDS International Center for Diffraction Data.
21. Aitasalo T, Hölsä J, Laamanen T, Lastusaari M, Lehto L, et al. (2006) Crystal structure of the monoclinic $Ba_2MgSi_2O_7$ persistent luminescence material. Zeitschrift fur Kristallographie Supplements, pp. 481-486.
22. Singh D, Sheoran S, Tanwar V (2017) Europium doped silicate phosphors: synthetic and characterization techniques. Advanced Materials Letters 8(5): 656- 672.
23. Gou Z, Chang J, Zhai W (2005) Preparation and characterization of novel bioactive di calcium silicate ceramics. Journal of the European Ceramic Society 25(9): 1507-1514.
24. Dubey SK, Sharma S, Diwakar AK, Pandey S (2021) Structural Characterization and Optical Properties of Monoclinic $Ba_2MgSi_2O_7$ (BMS) Phosphor. International Journal of Scientific Research in Physics and Applied Sciences 9(6): 81-85.
25. Frost RL, Bouzaid JM, Reddy BJ (2007) Vibrational spectroscopy of the sorosilicate mineral hemimorphite $Zn_4(OH)_2Si_2O_7{\cdot}H_2O$. Polyhedron 26(12): 2405- 2412.
26. Chandrappa GT, Ghosh S, Patil KC (1999) Synthesis and properties of Willemite, Zn_2SiO_4, and M^{2+}: Zn_2SiO_4 (M= Co and Ni). Journal of Materials Synthesis and Processing 7(5): 273-279.
27. Shannon RD (1976) Revised effective ionic radii and systematic studies of interatomic distances in halides and chalcogenides. Acta crystallographica section A: crystal physics, diffraction, theoretical and general crystallography 32(5): 751-767.
28. Pawade VB, Dhoble SJ (2013) Blue emission in Eu^{2+} and Ce^{3+} activated novel aluminates-based phosphors. Journal of luminescence 135: 318-322.
29. Pawade VB, Dhoble NS, Dhoble SJ (2012) Synthesis and characterization of Eu^{2+} activated $X_{12}Al_{10.6}Si_{3.4}O_{32}C_{l5.4}$ (X= Sr, Ca) phosphors. Journal of Luminescence 132(8): 2054-2058.
30. Komeno A, Uematsu K, Toda K, Sato M (2006) VUV properties of Eu-doped alkaline earth magnesium silicate. Journal of alloys and compounds 408: 871-874.
31. Sharma S, Dubey SK (2022) Importance of the Color Temperature in Cold White Light Emission of $Ca_2MgSi_2O_7$:Dy^{3+} Phosphor. JACSI 13(4): 80-90.
32. (1931) CIE. International Commission on Illumination. Publication CIE no. 15 (E- 1.3.1).
33. CIE Color Spaces - SPIE Book, Digital Library, DOI: 10.1117/3.660835.ch5.

ISSN: 2574-1241

DOI: 10.26717/BJSTR.2022.46.007294

Shashank Sharma. Biomed J Sci & Tech Res

This work is licensed under Creative *Commons* Attribution 4.0 License

Submission Link: https://biomedres.us/submit-manuscript.php

Assets of Publishing with us

- Global archiving of articles
- Immediate, unrestricted online access
- Rigorous Peer Review Process
- Authors Retain Copyrights
- Unique DOI for all articles

https://biomedres.us/